

# A combination of the Hashin-Shtrikman bounds aimed at modelling electrical conductivity and permittivity of variably saturated porous media

A. Brovelli<sup>1</sup> and G. Cassiani<sup>2</sup>

<sup>1</sup>Laboratoire de technologie écologique, Institut d'ingénierie l'environnement, Bâtiment GR, Station No. 2, Ecole Polytechnique Fédérale de Lausanne, CH-1015 Lausanne, Switzerland. E-mail: [alessandro.brovelli@epfl.ch](mailto:alessandro.brovelli@epfl.ch)

<sup>2</sup>Dipartimento di Geoscienze, Università di Padova, Via Giotto 1, 35127 Padova, Italy

Accepted 2009 October 9. Received 2009 October 8; in original form 2009 March 4

## SUMMARY

In this paper, we propose a novel theoretical model for the dielectric response of variably saturated porous media. The model is first constructed for fully saturated systems as a combination of the well-established Hashin and Shtrikman bounds and Archie's first law. One of the key advantages of the new constitutive model is that it explains both electrical conductivity—when surface conductivity is small and negligible—and permittivity using the same parametrization. The model for partially saturated media is derived as an extension of the fully saturated model, where the permittivity of the pore space is obtained as a combination of the permittivity of the aqueous and non-aqueous phases. Model parameters have a well-defined physical meaning, can be independently measured, and can be used to characterize the pore-scale geometrical features of the medium. Both the fully and the partially saturated models are successfully tested against measured values of relative permittivity for a wide range of porous media and saturating fluids. The model is also compared against existing models using the same parametrization, showing better agreement with the data when all the parameters are independently estimated. An example is also presented to demonstrate how the model can be used to predict the relative permittivity when only electrical conductivity is measured, or vice versa.

**Key words:** Electrical properties; Hydrogeophysics; Microstructures; Permeability and porosity.

## 1 INTRODUCTION

Many problems of environmental and geological interest are linked to the presence and flow of water and other fluids in porous media. The effective use of geophysical techniques to approach these problems is dependent on the availability of reliable constitutive laws. These models typically link the distribution of fluids in the pores to the bulk physical properties of the medium as measured at the field or laboratory scale. In recent years, electromagnetic methods, such as ground penetrating radar (GPR), time domain reflectometry (TDR) and electrical resistivity tomography (ERT) have been widely utilized in hydrogeology, civil engineering, etc. (Vereecken *et al.* 2002, 2005, 2006; Butler 2005; Rubin & Hubbard 2005). In these applications, the electromagnetic properties inferred at the field-scale are translated, via constitutive models, into quantities of practical interest, such as moisture content, solute concentration, petrophysical and geotechnical properties of the porous medium. Constitutive laws are often empirical equations recovered from fitting experimental data, for example, the well-known Topp *et al.* (1980) model. An alternative approach consists of using weighted averages of the electromagnetic properties of the constituents, such

as the 'Lichteneker–Rother (LR) equation' (Guéguen & Palciauskas 1994):

$$\varepsilon_b^\alpha = \sum_{i=1}^n \phi_i \varepsilon_i^\alpha, \quad (1)$$

where  $\varepsilon_b$  is the bulk relative permittivity of the porous medium,  $\phi_i$  and  $\varepsilon_i$  are, respectively, the volume fraction and the (complex) relative permittivity of the  $i$ th phase,  $n$  is the total number of phases of which the medium is composed and the exponent  $\alpha$  is a fitting parameter ( $-1 \leq \alpha \leq 1$ ). For  $\alpha = 0.5$ , eq. (1) reduces to the well-known Complex Refractive Index Model (CRIM) (Birchak *et al.* 1974; Wharton *et al.* 1980; Dobson *et al.* 1985; Heimovaara *et al.* 1994; Rubin & Hubbard 2005). The main advantages of the LR equation are its simplicity and the presence of fitting parameters ( $\varepsilon_s$  and  $\alpha$ ) that help to adequately match the experimental data. The LR mixing model (eq. 1) and particularly the CRIM are not purely arbitrary fitting relationships, but have also some physical justifications (Birchak *et al.* 1974; Zackri *et al.* 1998). Model parameters are however not clearly connected to the petrophysical properties of the medium, and their estimation might be difficult (Brovelli

& Cassiani 2008). More theoretically sound are methods based for example on effective medium or mean-field approximations (e.g. Wagner 1924; Bergman 1978; Sihvola & Kong 1988, 1989; Friedman 1997; Cosenza *et al.* 2003) and the volume averaging approach (e.g. Pride 1994). For example, Friedman (1998) proposed a constitutive relationship for unsaturated soils as a linear combination of two effective medium models. The constitutive equation of Friedman (1998) produces a reasonably good data fit for a number of cases (e.g. Miyamoto *et al.* 2005; Blonquist *et al.* 2006; Chen & Or 2006). More recently, the volume averaging approach was used by Linde *et al.* (2006) to further extend the expression of Pride (1994) for the dielectric response of soils, by accounting for the effect of variable water saturation. Although a convincing validation of the model of Linde *et al.* (2006) against experimental data is still missing, the proposed relationship is particularly attractive in that it models electrical conductivity and dielectric properties using the same parametrization, namely the electrical formation factor  $F$ , the cementation factor  $m$  and the saturation exponent  $n$ . These parameters depend on the geometrical properties of the pore-space geometry (e.g. Revil & Glover 1998; Revil & Cathles 1999). It can therefore be expected that models based on these parameters might provide additional information regarding the structure and topology of the porous medium. The impact of the pore-scale geometrical properties on both the electrical and dielectrical response of the porous medium has been investigated (Madden & Williams 1993; Jones & Friedman 2000; Robinson & Friedman 2001; Friedman & Robinson 2002). All these studies concluded that changes in particle distribution and size modify the tortuosity and connectivity of the pore-space and therefore the bulk response of the medium. It is also observed that these changes cannot be accounted for by porosity variations only.

The aim of this paper is to develop a new constitutive law for the electromagnetic response of saturated and unsaturated porous media, including the effect of the pore-scale geometrical features of the composite. The model is based on a linear interpolation of analytical and exact upper and lower bounds. The model involves only parameters that can be measured independently and are related to the description of other physical properties of a multiphase porous medium such as electrical conductivity. The proposed relationship is subsequently tested using experimental data taken from the literature, and model predictions in terms of the microgeometrical parameters (Archie's cementation factor and saturation exponent) are compared with those obtained from alternative constitutive models adopting the same parametrization and with literature values.

## 2 THEORETICAL BACKGROUND

The use of analytical expressions suitable to define bounds for certain properties of a mixture has been studied extensively (Hale 1976; Milton 1981; Tripp *et al.* 1998, and references therein). The key advantage of bounds is that they provide the exact possible range of variation for the property of interest, given the available information. For example, the Hashin & Shtrikman (1962) bounds that will be discussed and used in the following, provide the narrowest possible range without information regarding the topology and distribution of the phases, whereas the bounds proposed by Miller (1969) incorporate the spatial geometrical information in the form of a three-point correlation function. The Hashin & Shtrikman (1962) bounds have been used in a variety of application to estimate transport coefficients. Examples of successful relevant applications

are the prediction of the electrical conductivity of partially molten earth mantle (e.g. Waff 1974; Park & Ducea 2003; Park 2004), and the mechanical properties of soils and granular mixtures (e.g. Watt & Peselnick 1980). In this context, it has been shown that a combination of the upper and lower bounds can be used to estimate the expected bulk properties of the mixture, for example, the elastic constants (Hill 1952; Thomsen 1972; Watt & Peselnick 1980; Berryman 2005). In this work, we follow a similar strategy but, rather than taking the arithmetic or geometric mean of the upper and lower bounds—as done in some of the works mentioned above—we compute the bulk response of the mixture as a weighted average of the upper and lower bound. The weighting factor explicitly incorporates some information about the geometry and topology of the pore structure, and consequently we expect an improved estimate of the bulk transport coefficient.

### 2.1 Relationship between bulk electrical conductivity and permittivity of a porous medium

Due to the formal equivalence of the governing macroscale equations, transport processes in porous media can be modelled using a unified treatment (Berryman 1992, 2005; Pride 1994; Revil & Linde 2006). For example, the thermal conductivity  $\lambda$ , the electrical permittivity  $\varepsilon$  (under quasi-static conditions) and the low frequency electrical conductivity  $\sigma$  are described by similar boundary-value problems (Guéguen & Palciauskas 1994; Pride 1994):

$$\nabla \cdot (\lambda \nabla T) = 0 \quad (2)$$

$$\nabla \cdot (\varepsilon \nabla V) = 0 \quad (3)$$

$$\nabla \cdot (\sigma \nabla V) = 0, \quad (4)$$

where  $V$  is the electric potential and  $T$  the temperature. Indeed, while the boundary-value problem is identical in the case of thermal conductivity and permittivity (Revil 2000; Berryman 2005), the additional contribution to the total conductivity of the excess charge at the interface between water and grain minerals further complicates the problem for the effective electrical conductivity (Brovelli *et al.* 2005). The surface conductivity is mainly due to impurities (clays and oxides) lining the pores and to the presence of electrically charged complexes on the surface of the silica grains, and ultimately to excess of charge resulting from the electrical double layer at the solid–water interface. This additional contribution is usually quantified in terms of the specific surface conductivity  $\Sigma_s$  (Revil and Glover 1998; Brovelli *et al.* 2005).

The dielectric constant is in the high frequency limit less sensitive to interfacial phenomena, because the intensity of the two key mechanisms, dielectric loss and reduced permittivity of water bond to clay minerals, is very limited. In fact, in the high frequency limit the displacement of ions responsible for dielectric losses is limited. The decrease in permittivity of water bond to clay particles occurs because the water molecules in the diffuse layer are affected by the electrostatic forces that develop near the charged surface, and consequently their response to the external electrical field is modified and reduced. The resulting effect is that the dielectric constant of the water phase is locally reduced (Dobson *et al.* 1985; Dirksen & Dasberg 1993; Saarenketo 1998; Lesmes & Friedman 2005) and consequently the water content is under predicted. This effect is only visible in soils with a fine to very fine texture, and *ad hoc* strategies have been developed to account for this effect (Knoll

*et al.* 1995; Friedman 1998; Saarenketo 1998; Lesmes & Friedman, 2005).

For the applications of practical interest the frequency ranges considered allows us to use eqs (3) and (4), respectively. For real porous media, however, the treatment of electrical conductivity and dielectric constant differs also because (i) the contrast in material permittivity is small compared to that of electrical conductivity, (ii) the lowest value for permittivity is the permittivity of vacuum (that corresponds to a relative permittivity equal to 1), while electrically insulating materials (e.g. quartz) have negligible electrical conductivity. Nevertheless, the specific surface conductivity can be converted into an equivalent grain conductivity  $\sigma_s = 3\Sigma_s/R$  (Brovelli *et al.* 2005; Linde *et al.* 2006), where  $R$  is the typical length scale of the grains (for example, the average particle radius for porous media with non-uniform grain size distribution). As a result of this transformation, the boundary value problems of electrical conductivity and permittivity are similar, and a similar approach can be used (Linde *et al.* 2006). The idea of exploiting this similarity between the permittivity and electrical conductivity to model these two electromagnetic properties in a unified frame is not new. For example the model of Linde *et al.* (2006) was developed to motivate the assumption of structural similarity when performing joint inversion of ERT and GPR data.

The electrical conductivity of a fully saturated porous medium is often described using first Archie's (1942) law. Assuming a negligible surface conductivity (i.e.  $\sigma_f \gg \sigma_s$ , where  $\sigma_f$  is the electrical conductivity of the pore fluid), the bulk electrical conductivity of a porous medium ( $\sigma_b$ ) is expressed as

$$\sigma_b = \frac{\sigma_f}{F} = \frac{\sigma_f}{\phi^{-m}}. \quad (5)$$

This constitutive relationship describes the electrical conductivity of granular porous media as a function of the pore-fluid conductivity  $\sigma_f$ , the porosity  $\phi$  and the (electrical) cementation exponent  $m$ . This latter is a parameter that summarizes the microgeometrical properties of the pore-space affecting the electrical response of soils, such as tortuosity and pore connectivity. The geometrical parameter  $F$  is the electrical formation factor in the case of negligible surface conductance. In conditions of partial water saturation, that is, in the presence of an air phase, Archie's law is modified to include water saturation.

Even though Archie's law (eq. 5) was originally developed as a purely empirical model, theoretical justifications have been presented (Madden 1976; Sen *et al.* 1981). Sen *et al.* (1981) derived eq. (5) using a self-consistent differential effective medium approach. The Sen *et al.* (1981) model—often named Sen–Hanai–Bruggeman (SHB) equation—was developed to describe the complex dielectric response of granular porous media; an equivalent form of eq. (5) was derived for relative permittivity in the limit  $\varepsilon_s \rightarrow 0$ , where  $\varepsilon_s$  is the permittivity of the solid matrix. Due to the analogy between eqs (3) and (5), eq. (5) can consequently be adopted for permittivity if the underlying assumptions of Archie's equation are honoured, that is, the permittivity of the solid matrix is small compared to that of the fluid phase. Therefore, based on Archie's formulation, it is possible to write an approximate relationship between bulk electrical conductivity  $\sigma_b$  and permittivity  $\varepsilon_b$  of a porous medium that involves the properties ( $\sigma_f$  and  $\varepsilon_f$ ) of the saturating fluid

$$\frac{\sigma_b}{\sigma_f} = \phi^m = \left( \frac{\varepsilon_b}{\varepsilon_f} \right)_{\varepsilon_f \gg \varepsilon_s}. \quad (6)$$

## 2.2 Bounds for the electromagnetic properties of porous media

In order to develop the new constitutive model, we start by studying some of the existing theoretical bounds for bulk properties of porous media (e.g. electrical conductivity and permittivity). Exact bounds—named Wiener bounds—are recovered considering an equivalent porous medium composed of two materials (e.g. solid and fluid phases) arranged in layers, conserving the relative volume of each material. The two bounds are computed making the flux perpendicular or parallel to the layers, respectively. In the first case, the porous medium behaves like an electric circuit composed of resistances in series, in the second case of resistances in parallel. The configurations in series and in parallel correspond to the maximum and minimum resistance, respectively. Hashin & Shtrikman (1962) on the basis of a variational approach derived narrower bounds, although valid for statistically isotropic (at the macroscale) granular porous materials only (geological media, packing of beads, etc.). The upper bound is the effective permittivity of a microstructure of spherical grains, each coated by a shell of fluid. The ratio between the volume of each grain and the volume of coating shell is in the range  $\phi$  to  $(1 - \phi)$ . The fluid is completely interconnected and forms a percolation cluster, while the grains are isolated. The lower bound is computed by interchanging the two materials. For a two-phase mixture, the HS bounds have the following analytical forms:

$$\varepsilon_{\text{HSL}} = \varepsilon_s + \frac{\phi}{(\varepsilon_f - \varepsilon_s)^{-1} + \frac{1-\phi}{3\varepsilon_s}} \quad (7)$$

$$\varepsilon_{\text{HSU}} = \varepsilon_f + \frac{(1 - \phi)}{(\varepsilon_s - \varepsilon_f)^{-1} + \frac{\phi}{3\varepsilon_f}}. \quad (8)$$

The subscripts HSL and HSU refer to the case  $\varepsilon_f > \varepsilon_s$ , while in the opposite case (e.g. dry porous medium) the bounds are inverted. Fig. 1 shows the Wiener and HS bounds as a function of matrix permittivity. Both for the Wiener and HS bounds one can observe that

$$\left( \frac{\partial \varepsilon_b}{\partial \varepsilon_s} \right)_{\varepsilon_s \rightarrow \varepsilon_f} = 1 - \phi \quad (9)$$

and consequently

$$\frac{\partial \varepsilon_b}{\partial \varepsilon_s} \geq 1 - \phi. \quad (10)$$

This result is reported as being a general conclusion (Woodside & Messmer 1961): the derivative of the bulk permittivity with respect to a generic phase is always greater than or equal to the relative volume of the considered phase. As all the rigorous bounds have these properties, any equation that is adopted to model the permittivity should logically satisfy eq. (10). Note for instance that the LR model (eq. 1) satisfies such constraint for any value of  $\alpha$ .

## 3. MODEL DEVELOPMENT

### 3.1 Formulation of the new constitutive equation for saturated conditions

Our approach to developing a new constitutive relationship for the permittivity of porous media consists of finding a suitable combination of the HS bounds. Let us assume that the bulk permittivity  $\varepsilon_b$  of a porous medium can be represented as a linear combination of

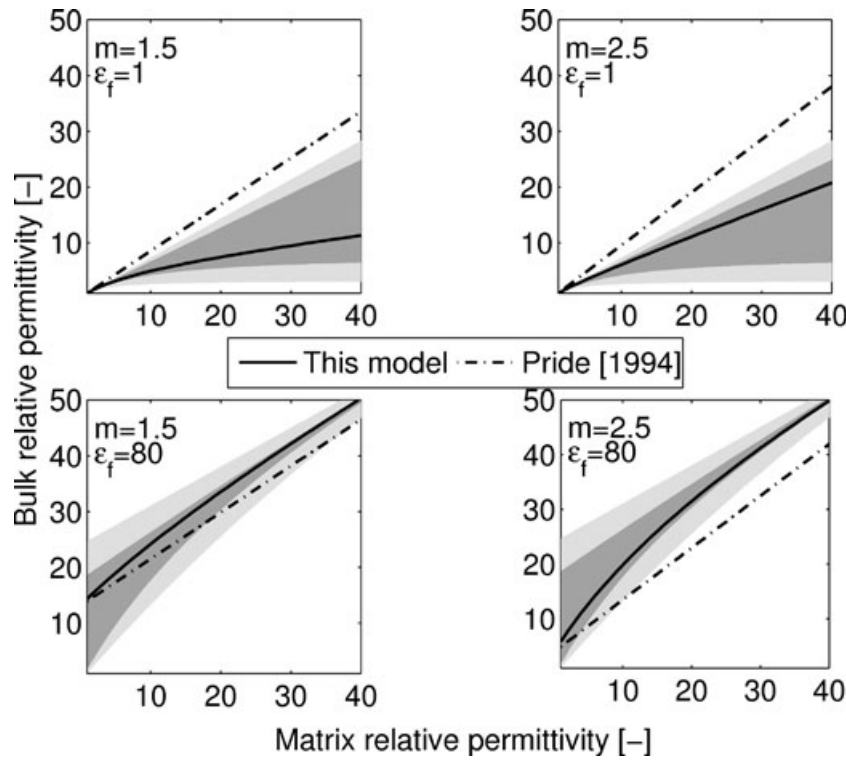


**Figure 1.** The proposed model (eq. 13) (solid line) compared to the ranges predicted by the Wiener (shaded area, light grey) and Hashin-Shtrickman bounds (shaded area, dark grey). The constitutive equation of Pride (1994) that uses the same parametrization is also shown for comparison. Porosity was set to 0.30 in all cases, while the cementation factor  $m$  and the fluid permittivity  $\varepsilon_f$  are varied to cover the range found in natural conditions.

the permittivities corresponding to the upper and lower HS bounds  $\varepsilon_{\text{HSL}}$  and  $\varepsilon_{\text{HSU}}$ , where  $\psi$  is for now an arbitrary weighting factor:

$$\varepsilon_b = \psi \varepsilon_{\text{HSU}} + (1 - \psi) \varepsilon_{\text{HSL}}. \quad (11)$$

Note that if we interpret  $\psi$  as the volume fraction of a material having permittivity  $\varepsilon = \varepsilon_{\text{HSU}}$  in a two-phase system, while the other material has permittivity  $\varepsilon = \varepsilon_{\text{HSL}}$ , eq. (11) corresponds to the permittivity of a system of phases connected in parallel. In order to identify an analytical expression for  $\psi$ , we now use eq. (6). Under the condition  $\varepsilon_f \gg \varepsilon_s$  (or  $\varepsilon_s/\varepsilon_f \rightarrow 0$ ),  $\varepsilon_{\text{HSL}} \rightarrow 0$  and eqs (8) and (11) can be combined

$$\psi_0 = \psi(\varepsilon_f \gg \varepsilon_s) = \frac{\varepsilon_f}{\varepsilon_{\text{HSU}}(\varepsilon_f \gg \varepsilon_s)\phi^{-m}} = \frac{3 - \phi}{2} \phi^{(m-1)}. \quad (12)$$

The resulting weighting factor  $\psi_0$  is a function of the geometrical factors only, namely the porosity  $\phi$  and Archie's cementation exponent  $m$ . Substituting eq. (12) into eq. (11) we obtain

$$\varepsilon_b = \frac{3 - \phi}{2} \phi^{(m-1)} \varepsilon_{\text{HSU}} + \left[ 1 + \frac{\phi - 3}{2} \phi^{(m-1)} \right] \varepsilon_{\text{HSL}}. \quad (13)$$

eq. (13) is the new constitutive equation we propose in this work to predict the dielectric response of two phase (solid matrix and a saturating fluid) granular porous media. The conditions described by eqs (9) and (10) are satisfied by eq. (13). The key assumption in the derivation of eq. (13) is that the weighting factor  $\psi$  computed in the limit  $\varepsilon_s/\varepsilon_f \rightarrow 0$  is used regardless the contrast between solid and fluid permittivity. The impact of this assumption is however only limited, because in the condition  $\varepsilon_s/\varepsilon_f \rightarrow 0$ , where our model is exact, the upper and lower HS bounds differ the most under the common condition that pore fluid (e.g. water) has permittivity higher than the solid matrix (see Fig. 1). Adopting  $\psi = \psi_0$  is therefore equivalent to having an exact weight at the condition where the

weight matters more ( $\varepsilon_f \gg \varepsilon_s$ ) and using this same value also at less critical values of  $\varepsilon_s$ . To say in a slightly different manner, as  $\varepsilon_s$  increases and the HS bounds get closer to each other, the impact of choosing a limiting value  $\psi_0$  has a progressively smaller influence on the value of eq. (13). This is visible in Fig. 1 where we compare the behaviour of eq. (13) (solid line) with the corresponding HS bounds (shaded area, dark grey), using two different values of pore-fluid permittivity and two cementation factors. The values of  $m$  and  $\varepsilon_s$  are chosen so as to cover the whole range that can be found in natural conditions. Instead, a large range of solid matrix permittivity is investigated although realistic (natural) values lay in the range 4.5–10, being 4.5 the permittivity of quartz and 13–15 the permittivity of shale (Guéguen & Palciauskas 1994). The two upper plots in Fig. 1 show the behaviour of the proposed model when the solid matrix permittivity is larger than (or equal to) the permittivity of the pore fluid, as for dry soils, while the lower graphs display the opposite case. All plots show that the allowed bulk permittivity range, as computed using the HS bounds, decreases as the permittivity of the solid matrix approaches that of the pore fluid.

### 3.2 Formulation of the new constitutive equation for variably saturated porous media

The HS bounds are not restricted to mixtures of two materials, but they can be applied to any composite with an arbitrary number of phases. It has however been observed that the HS bounds are optimal (i.e. provide the narrowest possible interval) only when the mixture contains only two phases (Talbot *et al.* 1995). Furthermore, it is possible to show that, as the volume fraction of one of the components in the assemblage (the phase with largest and smallest dielectric constants for the upper and lower bound, respectively)

becomes small and eventually reduce to 0, the  $n$ -phase HS bounds do not reduce to the equivalent bounds for  $(n - 1)$ -phases. This has been pointed out as a limitation of the approach adopted by Hashin & Shtrikman (1962) (Talbot *et al.* 1995). For our constitutive relationship, this would imply that the values estimated considering the two-phase HS bounds (at water saturation of 1.0 and 0.0) would be different from the same value estimated using the three-phase equivalent relationship. To avoid this inconsistency, we have developed an alternative approach that makes use of the two-phase bounds, since these are optimal. We consider porous materials made of a solid and a water phase, as for the two-component model discussed in the first part of this paper, and an additional non-aqueous phase (NAPL). This latter can be a gas phase (such as air) or a non-polar liquid nearly insoluble and immiscible in water (such as hydrocarbons, solvents, etc.). In contrast to the solid immobile phase (soil matrix), the water and non-aqueous phase will also be referred to as mobile phases in the following.

We compute the bulk permittivity of an unsaturated porous medium using the same constitutive model (13), but replacing the permittivity of the single fluid phase with that of the mixture of the 2 mobile phases filling the pore space,  $\varepsilon_p$

$$\varepsilon_b(\varepsilon_s, \varepsilon_p, \phi, s_w) = \psi \cdot \varepsilon_{\text{HSU}} + (1 - \psi) \cdot \varepsilon_{\text{HSL}}. \quad (14)$$

The permittivity  $\varepsilon_p$  of the pore fluid is a function of the relative amount and the permittivity of each phase, as well as of the geometrical distribution of the two mobile components within the pore space. For a given porous medium the spatial configuration of the saturating phases is a function of the pore fluid saturation, of the chemical and physical properties of the matrix surface (e.g. wettability) and of the two mobile phases (e.g. Knight & Abad 1995; Chen & Or 2006). In this work, we compute the bulk permittivity of the two-phase mixture filling the pore-space with a relationship similar to that we use for the two-phase porous medium

$$\varepsilon_p(\varepsilon_w, \varepsilon_{\text{NAPL}}, s_w) = w \cdot \varepsilon_{\text{HSU}}(\varepsilon_w, \varepsilon_{\text{NAPL}}, s_w) + (1 - w) \cdot \varepsilon_{\text{HSL}}(\varepsilon_w, \varepsilon_{\text{NAPL}}, s_w), \quad (15)$$

where  $w$  is the weight function, computed as

$$w = \frac{\varepsilon_w}{\varepsilon_{\text{HSU}} s_w^{-n_\varepsilon}}. \quad (16)$$

In eqs (15) and (16) porosity has been replaced by the degree of water saturation, and Archie's cementation factor with a permittivity saturation exponent  $n_\varepsilon$ , still to be defined in detail. The model for unsaturated porous media we propose in this work combines eqs (15) and (16) to compute the effective permittivity of the pore-space, which is subsequently used in eq. (13) to compute the bulk permittivity of the medium. The derived equation relies upon two main approximations: (i) we assume an exponential relationship between water saturation and bulk permittivity of the water/NAPL mixture filling the pore space and (ii) the weight function is exact when  $\varepsilon_w \gg \varepsilon_{\text{NAPL}}$  only, that is, the NAPL dielectric constant is much smaller than that of the water phase. In the frequency range we are considering, the dielectric constant of the water phase is always around 80, and it is only slightly affected by temperature and ionic strength. Instead, the dielectric constant of numerous NAPLs often found in natural and contaminated soils is small, including that of air (Table 1). Very often it is found that  $\varepsilon_w > 20\varepsilon_{\text{NAPL}}$ , thus the approximation at point (ii) is largely satisfied. Under the same approximation, the Hashin–Strickman lower bound reduces to 0 and eq. (15) simplifies to

$$\varepsilon_p(\varepsilon_w, s_w) = w \cdot \varepsilon_{\text{HSU}}(\varepsilon_w, s_w) = \varepsilon_w \cdot s_w^{n_\varepsilon}. \quad (17)$$

**Table 1.** Dielectric permittivity of some common non-aqueous phases found in natural and contaminated porous media, and used in this study.

Component	Dielectric constant [-]	Source
Air	1.00	Roth <i>et al.</i> (1990)
TCE	3.35	Ajo-Franklin <i>et al.</i> (2004)
Synthetic motor oil	2.66	Persson & Berndtsson (2002)
Sunflower seed oil	3.06	Persson & Berndtsson (2002)
$n$ -paraffin	2.32	Persson & Berndtsson (2002)

As discussed in Section 2, the electrical conductivity and the permittivity can be described by equivalent equations. Electrical conductivity of unsaturated porous media with negligible surface and matrix conductivity is commonly described using second Archie's law

$$\sigma_b(s_w) = \sigma_b(s_w = 1) \cdot s_w^n, \quad (18)$$

where  $\sigma_b(s_w)$  is electrical conductivity at water saturation level  $s_w$ ,  $\sigma_b(s_w = 1)$  is the electrical conductivity at full water saturation, and  $n$  is a geometrical factor named Archie's saturation exponent. The same relationship is often expressed using the resistivity index  $R$

$$R = \frac{\sigma_b(s_w)}{\sigma_b(s_w = 1)} = s_w^n. \quad (19)$$

We can re-write (15) to have an analogous form as (19), defining by analogy a permittivity index  $P$

$$P = \frac{\varepsilon_b(s_w)}{\varepsilon_b(s_w = 1)}, \quad (20)$$

where  $\varepsilon_b(s_w)$  is now the permittivity at a given water saturation level  $s_w$ , and  $\varepsilon_b(s_w = 1)$  is the permittivity at full water saturation. For the same analogy between permittivity and conductivity used in Section 2, we will from now on assume that  $n_\varepsilon$  in eq. (17) is the same as Archie's saturation exponent, that is, that  $n_\varepsilon = n$ . As previously discussed, the main assumption underlying the validity of the 1st Archie's law is that the electrical conductivity of the porous matrix is negligible. Using for now the same assumption for permittivity ( $\varepsilon_s = 0$ ), and combining (14) and (20) we obtain

$$P_{\varepsilon_s=0} = \frac{\varepsilon_b(\varepsilon_s = 0, s_w)}{\varepsilon_b(\varepsilon_s = 0, s_w = 1)} = \frac{\varepsilon_p(s_w)}{\varepsilon_p(s_w = 1)} \cdot \frac{\phi^{-m}}{\phi^{-m}} = \frac{\varepsilon_p(s_w)}{\varepsilon_w} \quad (21)$$

and finally combining (17) and (21) we obtain

$$P_{\varepsilon_s=0, \varepsilon_{\text{NAPL}}=0} = \frac{\varepsilon_w \cdot s_w^n}{\varepsilon_w} = s_w^n. \quad (22)$$

Two simplifying assumptions are required to reduce the dependence on saturation to eq. (22), that is, the permittivity of both the solid phase and of the non-aqueous phase are assumed to be small as compared to the permittivity of the water phase. This is largely correct for the non-aqueous phase permittivity, while it is only approximate for the solid matrix permittivity (recall that  $4.5 < \varepsilon_s < 6.5$  in natural porous media). Therefore, we can conclude that assuming that the permittivity saturation exponent is the same as the equivalent Archie's parameter introduces only a minor error. This conclusion has an important consequence for practical applications: measurements of the dependence of bulk electrical conductivity on water saturation can also provide reasonable estimates of the dielectric constant and vice versa.

3.3 Model comparison with existing constitutive equations

The model we have developed is a combination of eqs (13), (15) and (16). Eqs (15) and (16) are applied to recover the effective permittivity of the mixture of the mobile phases, which is subsequently inserted in eq. (13) to compute the bulk relative permittivity of the porous medium. In saturated conditions (two-phase systems) the model reduces to eq. (13) only, and the permittivity of the pore-space is replaced by that of the fluid phase. In three-phase conditions the model has two calibration parameters, the cementation factor  $m$  and the saturation exponent  $n$ , while for two-phase materials only  $m$  can be adjusted. An equivalent parametrization is used in the model proposed by Pride (1994) (two-phases) and Linde *et al.* (2006) (for three-phases). This constitutive law is recovered using a volume averaging approach. For unsaturated conditions, the bulk relative permittivity is computed as (Linde *et al.* 2006)

$$\epsilon_b = \frac{1}{F} [s_w^n \epsilon_b + (1 - s_w^n) \epsilon_a + (F - 1) \epsilon_s] \tag{23}$$

and the model for two-phases is recovered by setting  $s_w = 1$  in eq. (23). Since the same parameters are involved in our model and in eq. (23) (recall the formation factor is  $F = \phi^{-m}$ ), we have compared the behaviour of the two constitutive laws in a number of different cases, changing  $m$ ,  $n$ , porosity, matrix and fluid permittivities. Examples of this comparison are reported in Fig. 1 (for saturated porous media) and Fig. 2 (three phase materials). In Fig. 1, we also reported the expected intervals considering the Wiener (shaded area, light grey) and HS bounds (shaded, dark grey). From our sensitivity analysis, we have found that, for the same values of  $m$ ,  $n$  the two models have a different behaviour. Moreover, we have observed that, in some situations, eq. (23) falls outside the range predicted by the theoretical bounds (see for example, the left-hand panels of

Fig. 1). This indicates that the model of Pride (1994) and Linde *et al.* (2006) fails under some conditions. It is however not possible to determine from the results of this analysis whether the parameters (i.e.  $m$ ,  $n$ ) estimated by fitting eq. (23) or our model are correct. This will be done in the next section, although for the cementation factor only.

We have also investigated how our model compares against the well-known and widely adopted Topp and CRIM models for different values of the parameters. The permittivities of the three components were fixed ( $\epsilon_s = 5.5$ ,  $\epsilon_f = 80.0$  and  $\epsilon_a = 1.0$ ), while porosity was set to 0.35. Note however that Topp’s equation only depends on the water content, while the CRIM model also incorporates porosity and phase permittivities.

Fig. 3 shows that overall the three equations have a similar behaviour. Nevertheless, our model (solid line), thanks to its two adjustable parameters, shows a much greater flexibility. While the effective relative permittivity of the dry porous medium ( $s_w = 0$ ) is nearly the same for all cases and all models, different values of the cementation factor result in different permittivities at full water saturation ( $s_w = 1$ ). This cannot be reproduced by the CRIM and Topp model. This can only be achieved by adjusting the  $\alpha$  exponent of the CRIM equation, which is similar to changing the cementation factor  $m$ , as these two parameters are inversely correlated (Brovelli & Cassiani 2008). The saturation exponent  $n$  affects the slope of the water saturation—bulk permittivity proposed relationship. When the saturation exponent is set to 2 the proposed equation closely reproduces the behaviour of Topp and CRIM models. This is an interesting result, since both Topp and CRIM models often reproduce experimental data. Also, it is widely recognized that for the electrical conductivity—water saturation relationship the Archie’s saturation exponent is often close to 2 (Mualem & Friedman 1991; Schön 1996; Ewing & Hunt 2006). As the value of the  $n$  exponent

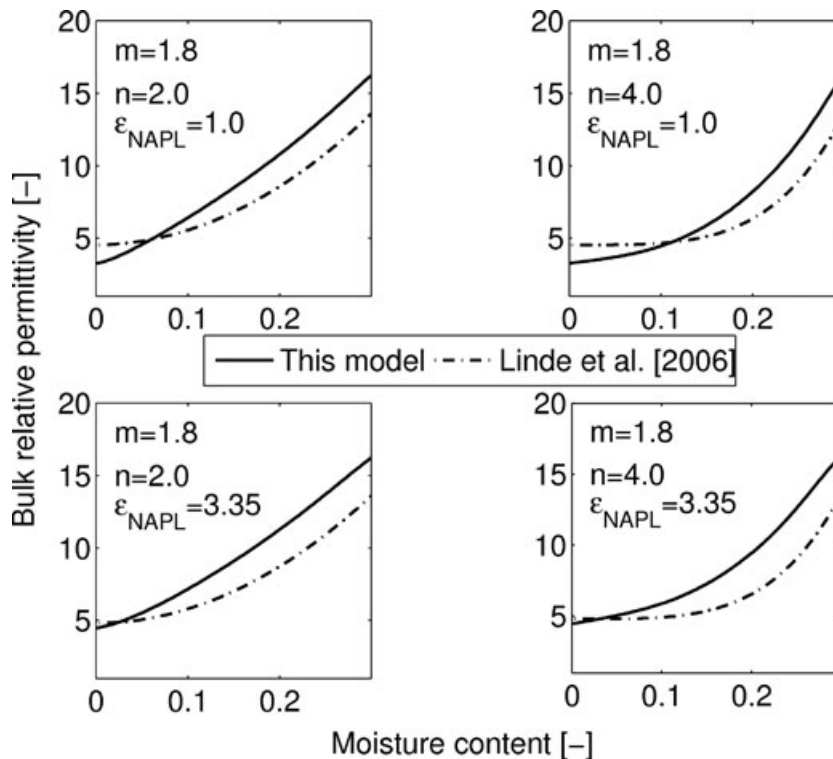
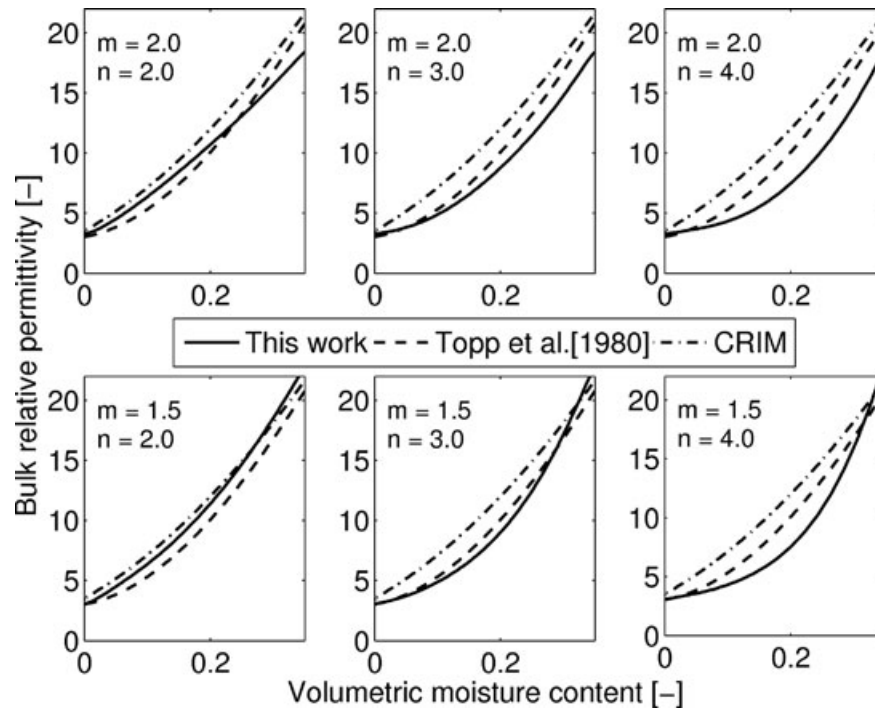


Figure 2. The proposed model (eqs 13, 15 and 16) (solid line) compared to the model of Linde *et al.* (2006). The two models use the same parametrization (Archie’s cementation factor  $m$  and saturation exponent  $n$ ) but the predicted bulk relative permittivity is substantially different.



**Figure 3.** Comparison of the proposed equation for multiphase porous media, that is, eqs. (15), (16) and (13) against the Topp *et al.* (1980) model, and the CRIM equation for different values of the model parameters. The proposed model is always similar to the other two models, but shows a greater flexibility. Porosity is set to 0.35 in all cases.

increases, the curvature increases, but the end point (at  $s\varepsilon_w = 1$ ) remains fixed, since this is only related to the cementation factor  $m$ . As discussed in the next section, different values for the saturation exponent  $n$  are likely to be related to different textures of the porous system. Note that neither the Topp nor CRIM model can accommodate changes in the curvature.

## 4 MODEL VALIDATION

### 4.1 Comparison with pore-scale simulations

The electrical simulator described in Dalla *et al.* (2004) and Brovelli *et al.* (2005) was adopted to compute the electrical conductivity and the permittivity of a digital porous medium consisting of a random sphere packing. The key advantage of using this simulator is that we can independently compute the formation factor of the packing (from simulation of the electrical conductivity) as well as its bulk permittivity. In order to compute the formation factor  $F$ , we conducted a suite of simulations varying the electrical conductivity of the water phase. From the resulting bulk electrical conductivity the formation factor  $F$  and Archie's cementation exponent  $m$  were easily computed. The digital porous medium we adopted had a porosity of 0.39 and a cementation exponent equal to 1.49. This latter value is very close to the 1.5 proposed by Sen *et al.* (1981) for sphere packings.

We subsequently computed the bulk permittivity of the digital porous medium varying its matrix permittivity. The fluid relative permittivity was kept constant and equal to 80, that is, the relative permittivity of water. Fig. 4 shows the pore-scale modelling results together with the proposed relationship, eq. (13) (solid line) and the constitutive model of Pride (1994) (dashed line). Our model closely matches the simulated data while Pride's (1994) model, using the same parameters, consistently underestimates the bulk permittivity. By adjusting the cementation factor it is possible to match the pore-

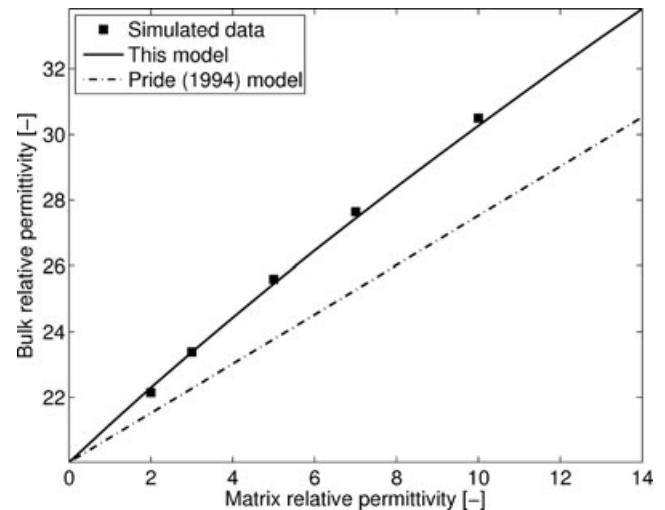


**Figure 4.** Comparison between the constitutive equations developed in this work and that of Pride (1994) with the pore-scale modelling data from Brovelli *et al.* (2005). All the model parameters are independently known and not fitted. Fluid permittivity is equal to 80, porosity 0.39 and the cementation factor  $m \approx 1.5$ .

scale results also with the model of Pride (1994). However, this only indicates that Pride's model, even when it provides a good match with experimental data, might fail to identify the correct governing parameters.

### 4.2 Comparison with experimental data in saturated conditions

After the successful validation with pore-scale modelling data, we tested our two-phase model against experimental data. To this end,

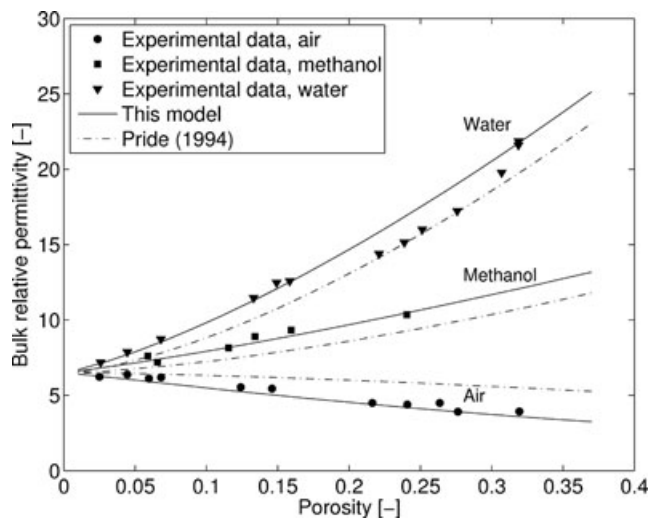


**Figure 5.** Comparison with the experimental data by Sen *et al.* (1981). The solid lines represent our proposed relationship (13), while the dashed lines show the predictions of Pride's (1994) model. The closed symbols are the experimental data. The cementation exponent  $m$  is not obtained by model fitting: the independently measured value obtained by Sen *et al.* (1981) is used. Consequently, no model parameter is adjusted to match the data. In nearly all the cases, Pride's (1994) model does not match the measurements without adjusting  $m$ .

we used the data sets reported by Sen *et al.* (1981) and Robinson & Friedman (2003). Sen *et al.* (1981) measured the complex bulk permittivity of glass bead packings as a function of porosity with three different saturating fluids: water ( $\epsilon_r = 80$ ), methanol ( $\epsilon_r = 30$ ) and air ( $\epsilon_r = 1$ ) (here the subscript  $r$  indicates the real component of the complex relative permittivity). Furthermore, Sen *et al.* (1981) measured the cementation exponent  $m$  of the porous media used in all experiments. The comparison with the model we propose and with the equation of Pride (1994) is depicted in Fig. 5. Eq. (13) reproduces satisfactorily the measured data, while the model of Pride (1994) under or overpredicts the experimental data, depending on whether the pore-space relative permittivity is larger or smaller than that of the skeleton. Since the cementation factor is independently estimated, eq. (13) predicts the experimental results making use of no fitting parameter, thus showing the predictive capabilities of the model, while eq. (23) is not able to reproduce the data without adjusting  $m$ .

Robinson & Friedman (2003) presented a suite of experiments where the bulk relative permittivity of numerous porous media is measured using different saturating fluids. We have tested the proposed model on this data set, estimating the cementation exponent by fitting eq. (13) to the data. Table 2 lists all the porous media we have used to validate the novel constitutive equation for two-phase conditions, together with the estimated values of the cementation factor. The determination coefficient ( $r^2$ ) and the root mean square error (RMSE) are the metrics we use to quantify the similarity between model predictions and observations. A visual comparison is also given in Fig. 6, where the measurements on glass spheres and silica sand (Robinson & Friedman 2003) are plotted together with the model. Overall, eq. (13) reproduces well all the experimental data reported in Robinson & Friedman (2003). Moreover, the cementation factors estimated from the fitting lie in the range 1–2.5, and compare very well with literature values for similar materials (Guéguen & Palciauskas 1994; Rubin & Hubbard 2005).

### 4.3 Comparison with variable-saturation experimental data

Following the validation of the equation in saturated conditions, we tested the model on three-phase, unsaturated porous materials. We considered a number of data sets that we divided in three different groups, depending on the soil properties and the non-aqueous phase liquid used in the measurements (air or non-polar organic liquid). Groups A and B (Paragraphs 4.3.1 and 4.3.2) are relevant to different types of porous media where the non-aqueous phase is air, while for Group C (Paragraph 4.3.3) the non-aqueous fluid is not air. For each data set, soil properties, measurement frequency, fitted parameters and goodness of fit measures are summarized in Table 3.

Inputs of our model are porosity, permittivity of the three phases, cementation factor  $m$ , and saturation exponent  $n$ . Porosity is known for all tested porous media (Table 3). Permittivity of water is set to 80, while the permittivity of the non-aqueous phase is set according to Table 1. On the contrary, the solid matrix permittivity is often unknown and needs to be estimated. In this work, we compute the permittivity of the solid matrix according to the mineralogical and chemical composition of the porous medium, thus reducing the number of parameters that must be adjusted to fit the experimental data. Although this approach may introduce some uncertainties, our numerical experiments show that model sensitivity to solid matrix permittivity is small and the approximation we introduce has in practice no impact. Consequently, in the following discussion only

**Table 2.** Validation of the two-phase proposed constitutive equation with data sets available in the literature.

Material	Reference	$\phi$	$\epsilon_s$	$m$	$r^2$	RMSE
Digital sphere packing	Brovelli <i>et al.</i> (2005)	0.39	5.0	1.49	>0.99	0.137
Glass beads, water	Sen <i>et al.</i> (1981)	–	6.5	1.5	0.99	0.223
Glass beads, methanol	Sen <i>et al.</i> (1981)	–	6.5	1.5	0.97	0.081
Glass beads, air	Sen <i>et al.</i> (1981)	–	6.5	1.5	0.99	0.193
Glass beads	Robinson & Friedman (2003)	0.39	7.6	1.4 <sup>a</sup>	>0.99	0.048
Quartz	Robinson & Friedman (2003)	0.38	4.7	1.5 <sup>a</sup>	>0.99	0.051
Soil	Robinson & Friedman (2003)	0.42	5.1	1.5 <sup>a</sup>	>0.99	0.045
Tuff	Robinson & Friedman (2003)	0.62	6.0	2.5 <sup>a</sup>	>0.99	0.075
Crushed sea shell	Robinson & Friedman (2003)	0.58	8.9	1.9 <sup>a</sup>	>0.99	0.076
Hematite	Robinson & Friedman (2003)	0.50	18.1	1.8 <sup>a</sup>	>0.99	0.109

*Notes:* Porosity and matrix relative permittivity are known for all the materials, while in some cases (noted with an <sup>a</sup>) the parameter  $m$  was calibrated to match experimental data. The proposed model well reproduces all the data sets considered, and the cementation factor, when estimated, is well within the expected range.

<sup>a</sup>This value was estimated to fit the experimental data.



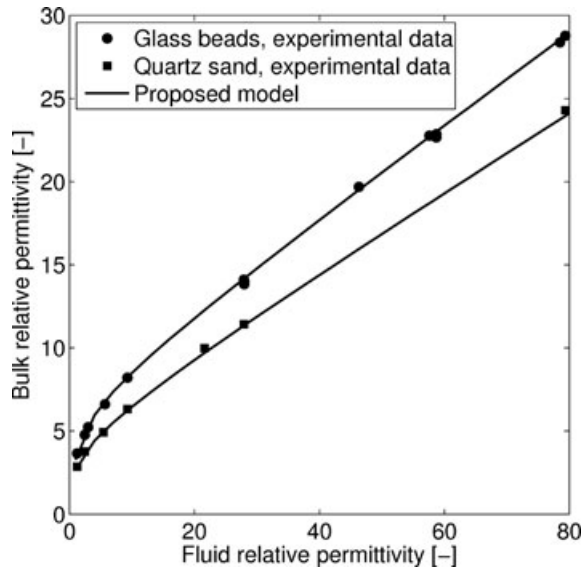


**Figure 6.** Comparison with the experimental data by Robinson & Friedman (2003). The solid lines are the proposed relationship (13), the dots are the experimental data. The cementation exponent  $m$  is here obtained by fitting the permittivity data. The model reproduces the data well in the whole range of fluid permittivity, as also indicated by the high correlation coefficients (Table 2).

the cementation factor and the saturation exponent are adjusted to fit the experimental data. The two parameters are tuned independently. First, the cementation factor  $m$  is adjusted to match observations at both saturated ( $\theta = \phi$ ) and dry conditions ( $\theta = 0$ ), where  $\theta$  is the volumetric moisture content. Next, the saturation exponent  $n$  is calibrated to fit the observations at intermediate degrees of water saturation.

4.3.1 Bulk permittivity of low clay content porous media

The first group of experimental data is composed of porous media with small or negligible clay content (Group A in Table 3), while

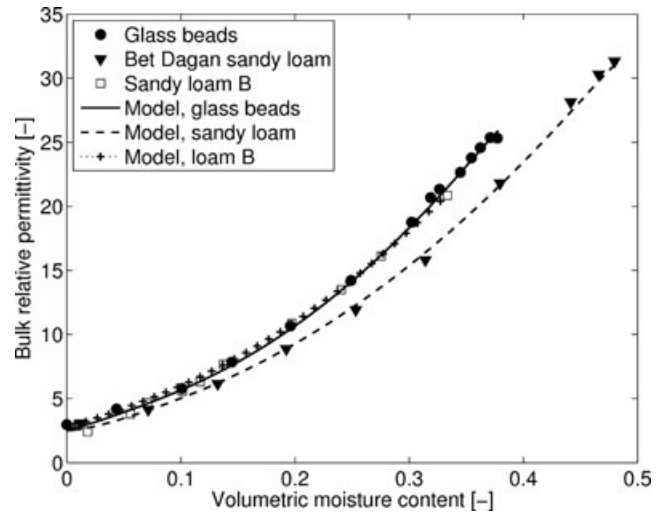


**Figure 7.** Comparison of the proposed equation with the experimental data of group A (negligible or low clay content), Table 3. Also in unsaturated conditions, the novel constitutive equation well reproduces the trend observed in the measurements.

the third phase is air. Comparison between the measurements and the calibrated model is shown in Fig. 7. The proposed model reproduces all the observations, as shown by the very high determination coefficient ( $r^2 > 0.99$ ) and low weighted residuals (RMSE < 0.5) for all three cases. The cementation factor is found to be about 1.5, which is a typical value for porous materials with rounded grains and negligible clay content (e.g. Lesmes & Friedman 2005). These materials are often named clean porous media, and are characterized by high pore connectivity, poorly cemented grains, and little content of clays and other fine components such as oxides. As already mentioned, theoretical results demonstrated that for glass beads (i.e. spherical grains) the expected value for the cementation factor is 1.5 (Sen *et al.* 1981). The saturation exponent is close to 2 for all three data sets. According to the literature (Mualem & Friedman 1991; Schön 1996; Ewing & Hunt 2006) this is a common value for

**Table 3.** Porous material used to validate the proposed equations.

Material	Source	$\omega$ (GHz)	$\phi$	$\epsilon_s$	$m^a$	$n^a$	$r^2$	RMSE
Group A – Low clay content								
Glass beads	Friedman (1998)	0.6	0.378	4.8	1.35	2.0	>0.99	0.33
Bet-Dagan sandy loam	Friedman (1998)	0.6	0.48	5.5	1.6	2.1	>0.99	0.41
Sandy loam B	Dobson <i>et al.</i> (1985)	1.4	0.334	5.0	1.5	2.0	>0.99	0.38
Group B – Dual porosity media								
Andisol 1	Miyamoto <i>et al.</i> (2005)	1.0	0.433	5.0	1.9	3.8	>0.99	0.47
Andisol 2	Miyamoto <i>et al.</i> (2005)	1.0	0.536	5.0	2.2	3.4	>0.99	0.67
Turfaco	Blonquist <i>et al.</i> (2006)	1.0	0.75	5.0	2.9	2.9	>0.99	1.32
Pumice	Blonquist <i>et al.</i> (2006)	1.0	0.83	5.0	3.5	3.5	>0.99	1.38
Profile	Blonquist <i>et al.</i> (2006)	1.0	0.74	6.0	2.8	2.8	0.99	1.44
Zeoponic	Blonquist <i>et al.</i> (2006)	1.0	0.61	6.0	1.6	2.0	>0.99	0.59
Group C – Organic phase								
Glass beads PB	Persson & Berndtsson (2002)	–	0.405	4.27	1.7	2.3	0.99	0.64
Sand, sample a	Ajo-Franklin <i>et al.</i> (2004)	–	0.39	5.0	1.65	1.80	0.97	0.23
Sand, sample b	Ajo-Franklin <i>et al.</i> (2004)	–	0.41	5.0	1.40	3.00	0.89	0.93
Sand, sample c	Ajo-Franklin <i>et al.</i> (2004)	–	0.44	5.0	1.50	1.80	0.96	0.61

Notes: The parameters  $m$  and  $n$  were calibrated to match experimental data. The solid permittivity was independently computed from porous medium mineralogy.

<sup>a</sup>This parameter was estimated to fit the experimental data.

Archie's saturation exponent of clean materials. As already pointed out, when the saturation exponent is set to 2 and the cementation factor is between 1.5 and 2, the proposed model has a behaviour very similar to that of Topp *et al.* (1980) and CRIM models. Since the Topp model was derived fitting a third order function to a large data set of soils it is expected to be representative of the average behaviour of media with small clay content.

4.3.2 Bulk permittivity of dual-porosity media

The second group of data (Group B in Table 3) consists of aggregated porous media showing a dual-porosity behaviour. Materials belonging to this class present a two-level granular structure, with aggregates of relatively large diameter composed of grains with smaller size. It is therefore possible to distinguish between inter- and intra-aggregate porosity, with intra-aggregate pores having larger radius, thus draining first. Experimental data and model predictions for this set of measurements are compared in Fig. 8. The proposed model correctly reproduces the data in Group B, with high determination coefficient ( $r^2 \approx 0.99$ ) and low RMSE.

For dual porosity media, the Topp model and the CRIM are often found to be inappropriate (Miyamoto *et al.* 2003, 2005; Blonquist *et al.* 2006). The reason is found in the different drainage behaviour compared to single porosity media. When soil starts drying, the large intra-aggregate pores drain first, while the interaggregate porosity remains fully saturated and drains at higher capillary pressure. This behaviour is reflected in the water saturation—dielectric constant function. At high values of water saturation the bulk permittivity changes quickly, while the rate of change  $d\epsilon_b/ds_w$  decreases as water saturation decreases (Miyamoto *et al.* 2003, 2005). A possible explanation is that the connectivity of the water phase between the aggregates strongly reduces and in turn the bulk response of the medium becomes less sensitive to the permittivity of the fluid phase. The constitutive equation we propose can replicate this behaviour, at least to some extent. Fig. 9 shows the rate of change (derivative) of bulk permittivity as a function of water saturation. Porosity was

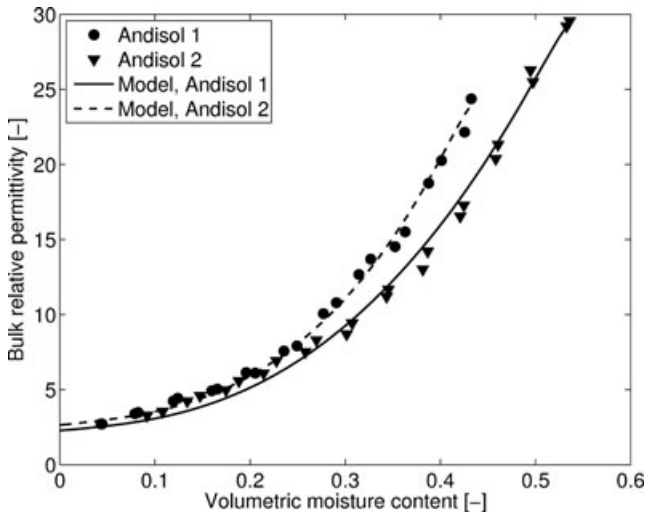


Figure 8. Comparison of the proposed model with the experimental data from Miyamoto *et al.* (2005). These data sets show a dual porosity behaviour and belong to group B in Table 3. Existing constitutive equations, such as the Topp *et al.* (1980) and CRIM, often fail for this class of porous materials. The proposed model instead can reproduce the behaviour observed in the experimental data by adjusting the value of the saturation exponent.

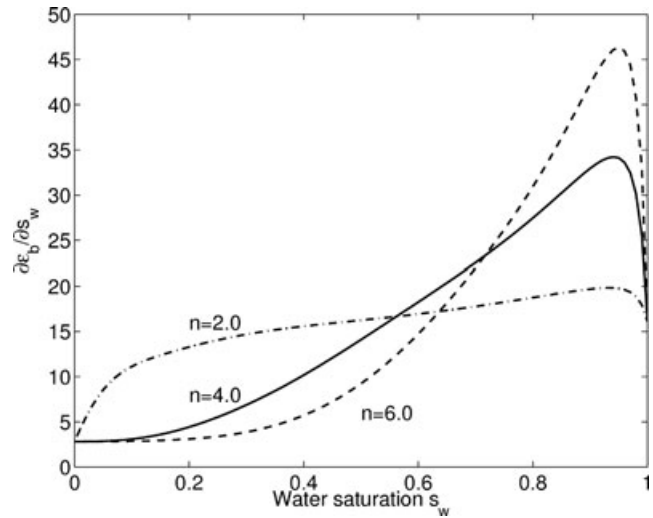


Figure 9. Derivative of the bulk permittivity with respect to water saturation for our proposed model. For different values of the saturation exponent, the derivative shows a completely different behaviour. This may explain some experimental observation for dual porosity (aggregate) materials.

set to 0.35 and the solid dielectric constant to 5.0. Clearly, different values of the saturation exponent result in a significantly different rate. For  $n = 2$ , starting from dry conditions, the rate quickly increases together with water saturation. For  $n = 4$  and  $n = 6$ , the rate is initially constant and only starts increasing at water saturation level higher than 0.1 and 0.2, respectively. It is also clear from Fig. 9 that the ‘threshold’ value of water saturation at which the rate starts changing is shifted towards higher values as the saturation exponent  $n$  increases. Calibrated parameters for Group B are consistent with these considerations. All but one of the materials have a high saturation exponent, compared to the average saturation exponent of the other groups. The exception is the saturation exponent of 2.0 for the material named ‘Zeoponic’. This is in agreement with the findings of Blonquist *et al.* (2006), which noted that experimental data of the permittivity–water saturation relationship for this material does not show a dual porosity behaviour, and can instead be correctly reproduced by Topp’s model.

Constitutive equations describing the water saturation—permittivity relationship, tailored to reproduce the behaviour of aggregated, dual porosity media have been recently developed (Miyamoto *et al.* 2005; Blonquist *et al.* 2006). The constitutive model we developed in this work differs from these models in that there is no clear transition from intra-aggregate to inter-aggregate porosity. For the Miyamoto *et al.* (2005) and Blonquist *et al.* (2006) models, the transition is marked by a discontinuity in the water saturation—permittivity function and by an abrupt change in its derivative. Instead, our equation shows a smooth continuous transition. Experimental data on aggregated materials show both behaviours. Of the six data sets we used in this work, three of them (Andisol 1, Andisol 2 and Zeoponic) show a gradual transition, while the remaining three (Turface, Pumice and Profile) show a marked change of the slope. We believe that the smooth transition behaviour arises when the water saturation of aggregates starts decreasing before the intra-aggregate porosity is completely drained. Therefore, the smooth change of the rate of variation is more typical of soils, which have a more complex inner geometry. The sharp change behaviour is instead restricted to a small number of porous media, with well-defined aggregates and a clear distinction between inter and intragranular porosity. We then conclude

that the model we propose is suitable for aggregated, dual porosity media. Although no quantitative relationship has been derived, we have shown that the saturation exponent can be used as an index to characterize the dual-porosity behaviour. Our conclusions are however preliminary and further investigations on a larger data set are required to confirm the findings.

#### 4.3.3 Bulk permittivity of samples with low clay content, water—organic phase mixture

The third set of data we considered (Group C, Table 3) is relevant to the dielectric properties of porous media partially saturated with a non-aqueous phase different from air, namely motor oil, seed oil and paraffin (Persson & Berndtsson 2002) and TCE (Ajo-Franklin *et al.* 2004)—see Table 1. All the NAPLs considered here are organic, non-polar substances. In the study performed by Persson & Berndtsson (2002) both electrical conductivity and permittivity were measured as a function of water saturation. This data set is therefore extremely interesting because it allows to test whether the model we have developed can be used to predict both the conductivity and relative permittivity of the same porous medium. In the first step both the cementation factor  $m$  and the saturation exponent  $n$  are computed by fitting Archie's model to the electrical conductivity curve (left-hand panel of Fig. 10). The fitted values are then used in a purely predictive manner in the proposed dielectric model, and the result is shown in Fig. 10, right panel, in comparison with the experimental data on permittivity of the same material. The result is highly satisfactory in terms of the predictive capabilities of our proposed model, showing that the model can be used for both the electromagnetic properties studied.

The proposed model was also compared with data from Ajo-Franklin *et al.* (2004), with the non-aqueous phase being TCE (Table 3). Again fitting was achieved by modifying only the cementation factor  $m$  and the saturation exponent  $n$ . The developed constitutive equation reproduces the behaviour of these other data set although with a slightly smaller correlation coefficient and higher residuals. This is possibly due to the method used during the experiments to inject the NAPL, or to modifications of the soil samples. Nevertheless, the overall fit is satisfactory and we can thus conclude that the proposed constitutive relationship is also suitable when the non-aqueous phase is an organic liquid.

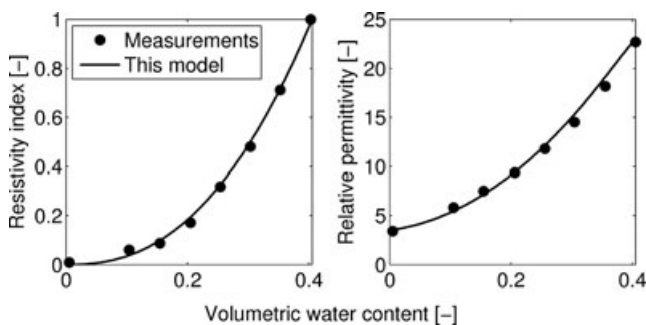


**Figure 10.** Comparison of our proposed model against the experimental data from Persson & Berndtsson (2002). This data set is extremely interesting in that it allows to test whether the model we propose can be used both for electrical conductivity and permittivity. In this example we have estimated the cementation factor and the saturation exponent on the electrical conductivity measurements, and applied the same values to predict the relative permittivity. The satisfactory comparison (see also the correlation coefficient in Table 2) further confirms the validity of the novel equation.

## 5 SUMMARY AND CONCLUSIONS

In this paper we presented a new constitutive model for the electromagnetic properties of multi-phase porous media, developed on the basis of the tightest theoretical bounds for transport properties (the Hashin–Shtrikman bounds) and the well known Archie's law, commonly used to describe the electrical conductivity of porous material. The model is consistently developed for two-phase (fully saturated) and three-phase (partially saturated) media on the basis of the same basic assumptions. For the sake of clarity, let us summarize the key model equations. First, the upper and lower HS bounds for two phases  $a, b$ , with volumetric fraction  $(1 - \phi)$ ,  $\phi$  are computed as

$$\varepsilon_{\text{HSL}}(\varepsilon_a, \varepsilon_b, \phi) = \varepsilon_a + \frac{\phi}{(\varepsilon_b - \varepsilon_a)^{-1} + \frac{1-\phi}{3\varepsilon_a}} \quad (24)$$

$$\varepsilon_{\text{HSU}}(\varepsilon_a, \varepsilon_b, \phi) = \varepsilon_b + \frac{(1 - \phi)}{(\varepsilon_a - \varepsilon_b)^{-1} + \frac{\phi}{3\varepsilon_b}}. \quad (25)$$

Using eqs (24) and (25), the bulk permittivity of the porous medium is

$$\varepsilon_b = \left[ \frac{3 - \phi}{2} \phi^{(m-1)} \right] \cdot \varepsilon_{\text{HSU}}(\varepsilon_s, \varepsilon_p, \phi) + \left[ 1 + \frac{\phi - 3}{2} \phi^{(m-1)} \right] \cdot \varepsilon_{\text{HSL}}(\varepsilon_s, \varepsilon_p, \phi), \quad (26)$$

where  $\phi$  is porosity,  $m$  the cementation factor,  $\varepsilon_s$  is the permittivity of the mineral solid matrix and  $\varepsilon_p$  is the permittivity of the pore space. For two-phase media, the permittivity of the pore-space is that of the mobile phase filling the pore space. For unsaturated systems instead,  $\varepsilon_p$  is computed from

$$\varepsilon_p(\varepsilon_w, \varepsilon_{\text{NAPL}}, s_w) = w \cdot \varepsilon_{\text{HSU}}(\varepsilon_w, \varepsilon_{\text{NAPL}}, s_w) + (1 - w) \cdot \varepsilon_{\text{HSL}}(\varepsilon_w, \varepsilon_{\text{NAPL}}, s_w), \quad (27)$$

where  $\varepsilon_{\text{NAPL}}$  is the permittivity of the non-aqueous phase liquid (air, oil, etc.),  $s_w$  is the degree of water saturation and  $w$  is the weight function,

$$w = \frac{\varepsilon_w}{\varepsilon_{\text{HSU}}(\varepsilon_w, 0, s_w) \cdot s_w^{-n}}. \quad (28)$$

To be consistent with Archie's law, our proposed model is applicable to media having a small clay fraction, since we exploited the similar role that pore-scale geometry, phase configuration and saturation state of the porous system have on the variation of electrical conductivity and permittivity as a function of water saturation. This similarity holds only for porous media with negligible surface conductivity.

The most important feature of the proposed model is its use of the same well-defined parameters for the description of both electrical conductivity and permittivity. This fact has important practical implications, as it makes it possible to infer the dielectric behaviour from the DC electric behaviour and vice versa for the same porous medium. Analogously, consistency between data on electrical conductivity and permittivity of the same medium can be checked on the basis of the proposed constitutive model. This might also be extremely useful for joint inversion, as discussed in Linde *et al.* (2006). The model has been tested successfully both against simulated data from pore scale models, and against experimental data from the literature, confirming its capability to explain within the same conceptual framework both the electrical conductivity and the permittivity of the same medium. A possible difficulty that might arise when applying the model at the field scale is that both the

cementation factor and the porosity have to be assumed or estimated by fitting the measurements. Since porosity while showing a moderate to high spatial variability is often measured only at very few locations, some care is necessary to evaluate the correlation between the two fitted parameters and the uncertainty associated to the estimated values.

A possible further development is the extension of the model applicability to media with significant clay fraction. This applicability has not been tested, but may still be acceptable. In the case of non-negligible surface conductivity, the same equations can be used to compute the cementation and saturation exponent, and in turn used to quantify the effect of surface conductivity. This may be useful, since constitutive equations linking the cementation factor to other effective properties of the porous medium have been proposed, such as the thermal and hydraulic conductivity.

## ACKNOWLEDGMENTS

This work was partly supported by the Consorzio Interuniversitario CINECA, by the Italian Ministry of Education, University and Research (MIUR) FIRB grant RBAU01TAL5 and COFIN grant 2005043992. Partial funding also came from the EU FP7 collaborative project iSOIL 'Interactions between soil related sciences—Linking geophysics, soil science and digital soil mapping'. The authors would like to acknowledge D. A. Robinson for providing some of the experimental data sets.

## REFERENCES

- Ajo-Franklin, J.B., Geller, J.T. & Harris, J.M., 2004. The dielectric properties of granular media saturated with DNAPL/water mixtures, *Geophys. Res. Lett.*, **31**, L17501, doi:10.1029/2004GL020672.
- Archie, G.E., 1942. The electrical resistivity log as an aid in determining some reservoir characteristics, *Trans. Am. Inst. Mining Met. Pet. Eng.*, **146**, 54–62.
- Bergman, D.J., 1978. The dielectric constant of a composite material. A problem in classical physics, *Phys. Rep. (Section C of Phys. Lett.)* **43**(9), 377–407.
- Berryman, J.G., 1992. Effective stress for transport properties of inhomogeneous porous rocks, *J. geophys. Res.*, **97**, 17 409–17 424.
- Berryman, J.G., 2005. Thermal conductivity of porous media, *Appl. Phys. Lett.*, **86**, 032905, doi:10.1063/1.1852718.
- Birchak, J.R., Gardner, C.G., Hipp, J.E. & Victor, J.M., 1974. High dielectric constant microwave probes for sensing soil moisture, *Proc. IEEE*, **62**(1), 93–98.
- Blonquist, J.M., Jr., Jones, S.B., Lebron, I. & Robinson, D.A., 2006. Microstructural and phase configurational effects determining water content: dielectric relationships of aggregated porous media, *Water Resour. Res.*, **42**, W05424, doi:10.1029/2005WR004418.
- Brovelli, A. & Cassiani, G., 2008. Effective permittivity of porous media: a critical analysis of the Complex Refractive Index Model, *Geophys. Prospect.*, **56**, 715–727.
- Brovelli, A., Cassiani, G., Dalla, E., Bergamini, F. & Pitea, D., 2005. Electrical properties of partially saturated sandstones: novel computational approach with hydrogeophysical applications, *Water Resour. Res.*, **41**, W08411, doi:10.1029/2004WR003628.
- Butler, D.K., Ed., 2005. *Near-Surface Geophysics, Investigations in Geophysics*, Vol. 13, Society of Exploration Geophysicists, Tulsa.
- Chen, Y. & Or, D., 2006. Geometrical factors and interfacial processes affecting complex permittivity of partially saturated porous media, *Water Resour. Res.*, **42**, W06423, doi:10.1029/2005WR004744.
- Cosenza, P., Camerlynck, C. & Tabbagh, A., 2003. Differential effective medium schemes for investigating the relationship between high-frequency relative dielectric permittivity and water content of soils, *Water Resour. Res.*, **39**(9), doi:10.1029/2002WR001774.
- Dalla, E., Cassiani, G., Brovelli, A. & Pitea, D., 2004. Electrical conductivity of unsaturated porous media: pore-scale model and comparison with laboratory data, *Geophys. Res. Lett.*, **31**, L05609, doi:10.1029/2003GL019170.
- Dirksen, C. & Dasberg, S., 1993. Improved calibration of time domain reflectometry soil water content measurements, *Soil Sci. Soc. Am. J.*, **57**, 660–667.
- Dobson, M.C., Ulaby, F.T., Hallikainen, M.T. & El-Rayes, M.A., 1985. Microwave dielectric behaviour of wet soils, II: dielectric mixing models, *IEEE Trans. Geosci. Remote Sens.*, **GE-23**, 35–46.
- Ewing, R.P. & Hunt, A.G., 2006. Dependence of the electrical conductivity on saturation in real porous media, *Vadose Zone J.*, **5**, 731–741.
- Friedman, S.P., 1997. Statistical mixing model for the apparent dielectric constant of unsaturated porous media, *Soil Sci. Soc. Am. J.*, **61**, 742–745.
- Friedman, S.P., 1998. A saturation degree-depend composite spheres model for describing the effective dielectric constant of unsaturated porous media, *Water Resour. Res.*, **34**, 2949–2961.
- Friedman, S.P. & Robinson, D.A., 2002. Particle shape characterization using angle of repose measurements for predicting the effective permittivity and electrical conductivity of saturated media, *Water Resour. Res.*, **38**(11), 1236, doi:10.1029/2001WR000746.
- Guéguen, Y. & Palciauskas, V., 1994. *Introduction to the Physics of Rocks*. Princeton University Press, Princeton, NJ.
- Hale, D.K., 1976. The physical properties of composite materials, *J. Math. Sci.* **11**, 2105–2141.
- Hashin, Z. & Shtrikman, S., 1962. A variational approach to the theory of the effective magnetic permeability of multiphase materials, *J. appl. Phys.*, **33**(10), 3125–3131.
- Heimovaara, T.J., Bouten, W. & Verstraten, J.M., 1994. Frequency domain analysis of time domain reflectometry waveforms. 2: a four component complex dielectric mixing model for soils, *Water Resour. Res.*, **30**(2), 201–209.
- Hill, R., 1952. The elastic behaviour of a crystalline aggregate, *Proc. Phys. Soc. Section A*, **65**(5), 349–354.
- Jones, S.B. & Friedman, S.P., 2000. Particle shape effects on the effective permittivity of anisotropic or isotropic media consisting of aligned or randomly oriented ellipsoidal particles, *Water Resour. Res.*, **36**, 2821–2833.
- Knight, R. & Abad, A., 1995. Rock/water interactions in dielectric properties: experiments with hydrophobic sandstones, *Geophysics*, **60**(2), 431–436.
- Knoll, M.D.R., Knight, R. & Brown, E., 1995. Can accurate estimates of permeability be obtained from measurements of dielectric properties? in *Proceedings of the Symposium on the Application of Geophysics to Environmental and Engineering Problems*, Environ. and Eng. Geophys. Soc., Orlando, FL.
- Lesmes, D. & Friedman, S.P., 2005. Relationships between the electrical and hydrogeological properties of rocks and soils, in *Hydrogeophysics*, eds Rubin, Y. & Hubbard, S.S., Springer, Amsterdam.
- Linde, N., Binley, A., Tryggvason, A., Pedersen, L.B. & Revil, A., 2006. Improved hydrogeophysical characterization using joint inversion of cross-hole electrical resistance and ground-penetrating radar traveltime data, *Water Resour. Res.*, **42**, W12404, doi:10.1029/2006WR005131.
- Madden, T.R., 1976. Random networks and mixing laws, *Geophysics*, **41**, 1104–1125.
- Madden, T. & William, E., 1993. Role of size distribution on physical properties: real size renormalization group, *J. geophys. Res.*, **98**(B9), 15 951–15 965.
- Miyamoto, T., Annaka, T. & Chikushi, J., 2003. Soil aggregate structure effects on dielectric permittivity of an Andisol measured by time domain reflectometry, *Vadose Zone J.*, **2**, 90–97.
- Miyamoto, T., Annaka, T. & Chikushi, J., 2005. Extended dual composite sphere model for determining dielectric permittivity of andisols, *Soil Sci. Soc. Am. J.*, **69**, 23–29.
- Miller, M.N., 1969. Bounds for the effective electrical, thermal, and magnetic properties of heterogeneous materials, *J. Math. Phys.*, **10**(11), 1988–2004.
- Milton, G.W., 1981. Bounds on the complex permittivity of a two-component composite material, *J. appl. Phys.*, **52**(8), 5286–5293.

- Mualem, Y. & Friedman, S., 1991. Theoretical prediction of electrical conductivity in saturated and unsaturated soil, *Water Resour. Res.*, **27**(10), 2771–2777.
- Park, S.K., 2004. Mantle heterogeneity beneath eastern California from magnetotelluric measurements, *J. geophys. Res.*, **109**, B09406, doi:10.1029/2003JB002948.
- Park, S.K. & Ducea, M.N., 2003. Can in situ measurements of mantle electrical conductivity be used to infer properties of partial melt? *J. geophys. Res.*, **108**(B5), 2270, doi:10.1029/2002JB001899.
- Persson, M. & Berndtsson, R., 2002. Measuring nonaqueous phase liquid saturation in soil using time domain reflectometry, *Water Resour. Res.*, **38**(5), 1064, doi:10.1029/2001WR000523.
- Pride, S., 1994. Governing equations for the coupled electromagnetics and acoustics of porous media, *Phys. Rev. B*, **50**, 15 678–15 696.
- Revil, A. & Linde, N., 2006. Chemo-electromechanical coupling in microporous media, *J. Coll. Int. Sci.*, **302**(2), 682–694.
- Revil, A., 2000. Thermal conductivity of unconsolidated sediments with geophysical applications, *J. geophys. Res.*, **105**(B7), 16 749–16 768.
- Revil, A. & Cathles, III, L.M., 1999. Permeability of shaly sands, *Water Resour. Res.*, **35**(3), 651–662.
- Revil, A. & Glover, P.W.J., 1998. Nature of surface electrical conductivity in natural sands, sandstones and clays, *Geophys. Res. Lett.*, **25**(5), 691–694.
- Robinson, D.A. & Friedman, S.P., 2001. Effect of particle size distribution on the effective dielectric permittivity of saturated granular media, *Water Resour. Res.*, **37**(1), 33–40.
- Robinson, D.A. & Friedman, S.P., 2003. A method for measuring the solid particle permittivity or electrical conductivity of rocks, sediments, and granular materials, *J. geophys. Res.*, **108**(B2), 2076, doi:10.1029/2001JB000691.
- Roth, K., Schulin, R., Fluher, H. & Attinger, W., 1990. Calibration of time domain reflectometry for water content measurement using a composite dielectric approach, *Water Resour. Res.*, **26**(10), 2267–2273.
- Rubin, Y. & Hubbard, S.S., eds, 2005. *Hydrogeophysics*, Springer, Amsterdam.
- Saarenketo, T., 1998. Electrical properties of water in clay and silty soils, *J. appl. Geophys.*, **40**, 73–88.
- Schön, J.H., 1996. *Physical Properties of Rocks: Fundamentals and Principles of Petrophysics*, Vol. 18: Seismic Exploration, Pergamon/Elsevier, Oxford, UK.
- Sen, P.N., Scala, C. & Cohen, M.H., 1981. A self-similar model for sedimentary rocks with application to the dielectric constant of fused glass beads, *Geophysics*, **46**(5), 781–795.
- Sihvola, A. & Kong, J.A., 1988. Effective permittivity of dielectric mixtures, *IEEE Trans. Geosci. Remote Sens.* **26**, 420–429.
- Sihvola, A. & Kong, J.A., 1989. Correction to Effective permittivity of dielectric mixtures, *IEEE Trans. Geosci. Remote Sens.* **21**, 101–102.
- Talbot, D.R.S., Willis, J.R. & Nesi, V., 1995. On improving the Hashin-Shtrikman bounds for the effective properties of three-phase composite media, *IMA J. appl. Math.*, **54**(1), 97–107.
- Thomsen, L., 1972. Elasticity of polycrystals and rocks, *J. geophys. Res.*, **77**(2), 315–327.
- Topp, G., Davis, J. & Annan, A., 1980. Electromagnetic determination of soil water content: measurement in coaxial transmission lines, *Water Resour. Res.*, **16**(3), 574–582.
- Tripp, A.C., Cherkava, E. & Hulen, J., 1998. Bounds on the complex conductivity of geophysical mixtures, *Geophys. Prospect.*, **46**, 589–601.
- Vereecken, H., Kemna, A., Münch, H.-M., Tillmann, A. & Verweerd, A., 2005. Aquifer characterization by geophysical methods, in ed., Anderson, M.G., pp. 2265–2283, *Encyclopedia of Hydrological Sciences*, John Wiley and Sons Ltd., Chichester.
- Vereecken, H., Binley, A.M., Cassiani, G., Revil, A. & Titov, K. eds, 2006. *Applied Hydrogeophysics*, Springer, Dordrecht.
- Waff, H.S., 1974. Theoretical considerations of the electrical conductivity in a partially molten mantle and implications for geothermometry, *J. geophys. Res.*, **79**(26), 4003–4010.
- Watt, J.P. & Peselnick, L., 1980. Clarification of the Hashin-Shtrikman bounds on the effective elastic moduli of polycrystals with hexagonal, trigonal and tetragonal symmetries, *J. appl. Phys.* **51**(3), 1525–1531.
- Wagner, K.W., 1924. Erklärung der Dielectrischen Nachwirkungsvorgänge auf grund Maxwellscher vorstellungen, *Archiv Electrotechnik*, **2**, 371–387.
- Wharton, R.P., Hazen, G.A., Rau, R.N. & Best, D.L., 1980. Electromagnetic propagation logging: advances in technique and interpretation, *Soc. Petrol. Eng.*, Pap. No. 9267, doi:10.2118/9267-MS.
- Woodside, W. & Messmer, J.H., 1961. Thermal conductivity of porous media. I: unconsolidate sands, *J. appl. Phys.*, **32**(9), 1688–1699.
- Zakri, T., Laurent, J.-P. & Vauclin, M., 1998. Theoretical evidence for ‘Lichtenecker’s mixture formulae’ based on effective medium theory, *J. Phys. D: appl. Phys.*, **31**, 1589–1594.